any particle that satisfies the criterion to be unlimited, i.e., once the particle enters the viscous sublayer it continues to move until it hits the wall.

References

[1]Lamb, H., *Hydrodynamics*, 6th ed., Cambridge University Press, Cambridge, England, 1932.

[2]Saffman, P. G., "The Lift on a Small Sphere in a Slow Shear Flow," *Journal of Fluid Mechanics*, Vol. 22, 1965, p. 385.

[3]Moore, D. W. and Saffman, P. G., "The Rise of a Body Through a Rotating Fluid in a Container of Finite Length," *Journal of Fluid Mechanics*, Vol. 31, 1968, p. 635.

[4]Rubinow, S. I. and Keller, J. B., "The Transverse Force on a Spinning Sphere Moving in a Viscous Fluid," *Journal of Fluid Mechanics*, Vol. 11, 1961, p. 447.

[5]Friedlander, S. K. and Johnston, H. F., "Deposition of Suspended Particles from Turbulent Gas Streams," *Industrial and Engineering Chemistry*, Vol. 49, 1957, p. 1151.

[6]Davies, C. N., "Deposition of Aerosoles from Turbulent Flow through Pipes," *Proceedings of the Royal Society of London*, Ser. A, Vol. 289, 1966, p. 235.

Computation of Unsteady Transonic Aerodynamics with Truncation Error Injection

K.-Y. Fung* and J.-K. Fu†
University of Arizona, Tuscon, Arizona

Introduction

THE urgent need for effective, reliable methods for unsteady aerodynamic predictions at transonic Mach numbers is evident from the Farmer and Hanson[1] experiment in which it was observed that the flutter boundary for a wing with a supercritical cross section is substantially lower than that with a conventional one. At transonic speeds, the size and location of the embedded supersonic zone over the wing affect the way acoustic signals propagate and, hence, the aerodynamic responses to disturbances. Recent developments in computational fluid dynamics and the availability of supercomputers have made accurate flow prediction possible. However, for applications like routine flutter calculation and aircraft design optimization, the currently available codes, especially the ones for three-dimensional computations like XTRAN3S of Rizzetta and Borland[2] and USTF3 of Isogai and Suetsugu,[3] are still much too time consuming.

As mentioned in Fung,[4] one of the problems in unsteady transonic flow computation is the grid for obtaining the solution. Aside from the issue of finding the best grid for a given wing geometry, a grid must have a local mesh size comparable to the radius of curvature of the leading edge in order to properly resolve the fast expansion that determines the size of the sonic bubble and the strength and location of the shock. The computational domain must be large enough to allow the flow to relax to the freestream condition with little confinement from grid boundaries. Almost all grids currently used for aerodynamic computations are based on these considerations. However, these grids, while suitable for computing steady flows, may require (due to linear or nonlinear numerical instability) too small a time-step limitation for efficient computations of the unsteady acoustic waves due to the small unsteady wing motions and deformations assumed in flutter analysis. For low-to-moderate reduced frequencies, the typical wavelength of an acoustic signal in a transonic flow is of the order of the chord of the wing. Hence, a grid with a minimum spacing of a tenth of the chord should be sufficient. However, an accurate prediction of the steady flowfield over a wing at supercritical Mach number often requires a minimum spacing of a hundredth of the chord and, hence, a time-step requirement based on the CFL condition 10 times as restricted as that needed for accuracy.

In this Note, a technique is introduced that allows the steady and unsteady flows to be computed on different grids. To demonstrate the efficiency of this technique, the unsteady small-disturbance transonic equation is used for unsteady aerodynamic prediction. The results of applying this technique are compared to those obtained on single grids.

Computations with Truncation Error Injection

It has been shown[5] that, by solving the corresponding difference equation with the truncation error included as a forcing term, exact nodal values of the solution to a differential equation can be obtained; that if the exact solution were known, the exact truncation error can be computed at nodal points; and that the truncation error can be approximated by local grid refinement.

Consider a difference equation of the form

$$L_t\phi_h + L_h\phi_h = 0 \tag{1}$$

where L_t and L_h correspond to the temporal and spatial discrete operators, respectively, and ϕ_h the numerical solution on a grid of size h. Assuming that ϕ_h^0 is the steady-state solution of Eq. (1) satisfying

$$L_h\phi_h^0 = 0 \tag{2}$$

it is quite obvious that ϕ_h also satisfies

$$L_t\phi_h + L_h\phi_h = L_h\phi_h^0 \tag{3}$$

and that solving Eq. (3) for ϕ_h is the same as solving Eq. (1). However, Eq. (3) is more general in the sense that, if it converges, it will yield the steady state ϕ_h^0 regardless of whether ϕ_h^0 satisfies Eq. (2). For example, we could replace ϕ_h^0 by $\phi_{h/N}^0$, i.e.,

$$L_t\phi_h + L_h\phi_h = L_n\phi_{h/N}^0 \tag{4}$$

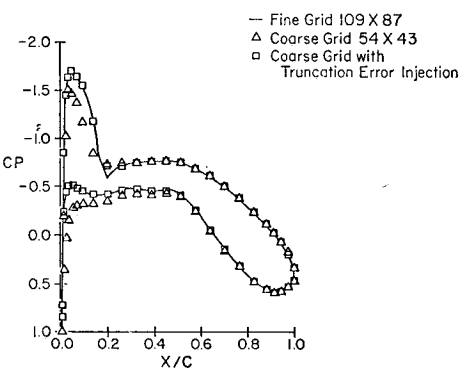

Fig. 1 Comparison of the surface pressure distributions of an NLR 7301 airfoil at $M_\infty = 0.70$ obtained by different methods on different grids.

Presented as Paper 85-1644 at the AIAA 18th Fluid Dynamics, Plasmadynamics and Lasers Conference, Cincinnati, OH, July 16-18, 1985; received Feb. 17, 1986; revision received Aug. 21, 1986. This paper is declared a work of the U.E. Government and is not subject to copyright protection in the United States.

*Associate Professor, Aerospace and Mechanical Engineering. Member AIAA.

†Research Assistant, Aerospace and Mechanical Engineering.

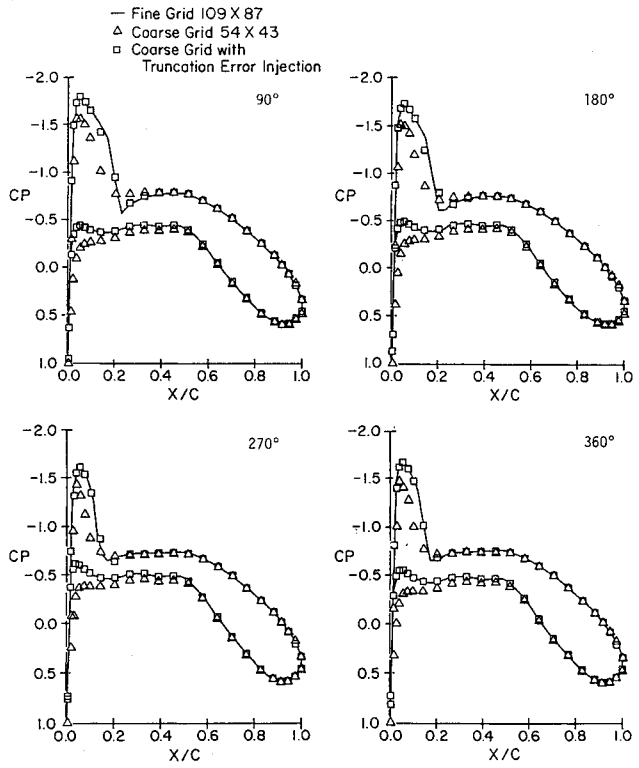

Fig. 2 Comparison of the unsteady pressure distributions (four intervals of a cycle) of an NLR 7301 airfoil pitching harmonically at $M_\infty = 0.70$ and at reduced frequency $k = 0.1$ obtained by different methods on different grids.

Table 1 Comparison of computation time for different computations, CPU's

	NACA-64A-010			NLR 7301		
Case	Steady	Unsteady	Total	Steady	Unsteady	Total
Fine grid	13.2	299.1	312.3	32.9	899.5	932.4
Coarse grid	5.5	14.5	20.0	10.4	56.5	66.9
Coarse + TEI	17.0	16.3	33.3	36.7	59.3	96.0

Here, $\phi^0_{h/N}$ denotes the steady-state solution on a finer grid of size h/N, satisfying the difference equation

$$L_{h/N}\phi^0_{h/N} = 0 \tag{5}$$

As explained in Fung et al.,[5] the term $L_h\phi^0_{h/N}$ in Eq. (4) is an approximation to the truncation error resulting from a Taylor's series expansion of the differential equation that Eq. (1) is modeling. The difference between Eqs. (3) and (4) is that the latter contains an approximation of the truncation error of the steady solution due to discretization and hence will yield the more accurate $\phi^0_{h/N}$ as a steady solution if, of course, the unsteady effects are allowed to diminish. Assuming that the base grid of size h is fine enough for resolving the unsteady part of ϕ_h, there will be very little or no truncation error due to discretization and Eq. (4) should yield more accurate solutions that Eq. (1).

In the case where the spatial operator L_h is linear, Eq. (4) is simply Eq (1) with the term $L_h\phi^0_{h/N}$ added to both sides of it. For nonlinear operators, Eq. (4) will enforce the perturbations about a steady state to satisfy the governing equation. It is of interest to note that the splitting of an operator into a steady and an unsteady operator as in Eq. (1) is necessary only for the clarity of the discussion.

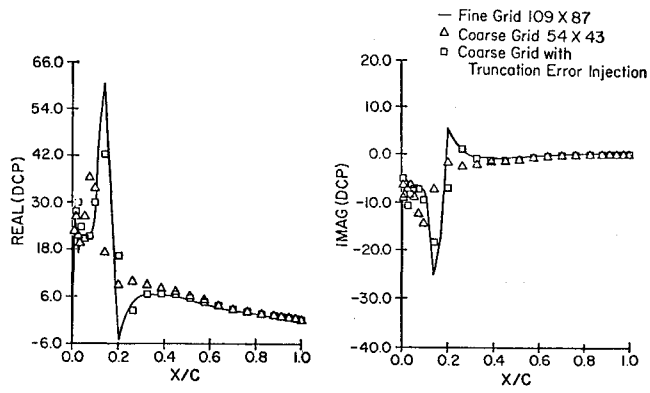

Fig. 3 Real and imaginary parts of the unsteady pressure distribution of an NLR 7301 airfoil pitching harmonically at $M_\infty = 0.70$ and at reduced frequency $k = 0.1$ obtained by different methods on different grids.

Numerical Example

To demonstrate its effectiveness, we have implemented this technique into the code AZTRAN[4] for solving the unsteady transonic small-disturbance equation. No modification to the code is needed except adding the stored truncation error values computed from the steady-state solution to the matrix equations at each time step. Figure 1 shows different steady-state pressure distributions for an NLR 7301 airfoil at a freestream Mach number $M_\infty = 0.70$ obtained on a fine grid (109×87) and on a coarse grid (54×43) that was formed by omitting every other grid line of the fine grid. As a result of faster expansion at the leading edge, the pressure distribution (solid line) obtained on the finer grid shows a stronger shock located further downstream compared to that (triangles) obtained on the coarser grid. The pressure distribution shown by the squares was obtained on the coarse grid with injected truncation error computed from the fine-grid solution. It coincides with the solid line almost everywhere except near the shock, where a smearing of the pressure jump occurs mainly because of numerical differentiation and graphic interpolation. The numerical smearing of the shock within one grid point, however, is of secondary importance as far as the computation of integrated loads for an aeroelastic application is concerned. Theoretically, unsteady perturbations on a shock create a singularity, an integrable one, however, in the perturbed quantities at the mean shock position. In reality, this singularity is often smeared by viscous effects. Motions of the shock, a nonlinear phenomenon in nature, also cause higher harmonics in the aerodynamic forces. However, it was shown by Davis and Malcolm[6] that the higher harmonics have little effect on the integrated loads.

Corresponding unsteady pressure distributions at 90-deg intervals for the same airfoil pitching harmonically at a reduced frequency $k = 0.1$ are shown in Fig. 2 and their first harmonic decompositions in Fig. 3. It is evident from these comparisons that, except for the minor differences near the shock, the results, including the motions of the shock, obtained on the coarse grid with truncation error injection are just as accurate as those on the fine grid. The CPU time, as listed in Table 1, for obtaining five cycles of harmonic motion on the fine grid was 900 s, for the coarse grid solution it was 57 s, and for the coarse grid solution with the truncation error injection it was 60 s. A reduction in computation time by a factor of four is attributed to the reduction in grid points and another factor of four to the relaxation of the allowable time step imposed by numerical stability.

Similar results for a conventional airfoil, NACA-64A-010, at a freestream Mach number of 0.796 and a reduced frequency of 0.1 are also listed in Table 1. Because of the conventional leading-edge shape, the pressure expansion at the leading edge is quite mild compared to that of the NLR 7301. Hence, the results obtained on both grids were just as accurate, except near the shock, with or without the truncation

error injection. This verifies an assumption in our theory that a relatively coarse grid is sufficient for resolving the unsteady acoustic waves if the steady pressure is accurate.

Conclusion

A simple numerical technique which can be easily implemented in any numerical code for computations of two- or three-dimensional unsteady transonic aerodynamics has been introduced. This technique allows the decoupling of a solution having two distinct length scales into two parts. By solving each part on a grid of the proper length scale, substantial savings in computation time and storage can be achieved.

Acknowledgments

This research was carried out at the Computational Fluid Mechanics Laboratory of the Aerospace and Mechanical Engineering Department under U.S. Air Force Office of Scientific Research Grant 83-0071, monitored by Dr. James D. Wilson, and NASA CFD Traineeship Grant NGT 03-002-800. Permission from Dr. Paul Kutler to use the NASA Ames Cray-XMP computer for this and other studies related to the traineeship program is gratefully acknowledged.

References

[1]Farmer, M.G. and Hanson, P.N., "Comparison of Supercritical and Conventional Wing Flutter Characteristics," *Proceedings AIAA/ASME/SAE 17th Structures, Structural Dynamics and Materials Conference*, King of Prussia, PA, April 1976, pp. 608–611 (see also NASA TMX-72837, May 1976).

[2]Rizzetta, D.P. and Borland, C.J., "Unsteady Transonic Flow Over Wings Including Viscous/Inviscid Interaction," *AIAA Journal*, Vol. 21, 1983, pp. 363–371.

[3]Isogai, K. and Suetsugu, K., "Numerical Calculation of Unsteady Transonic Potential Flow over Three-Dimensional Wings with Oscillating Control Surfaces," *AIAA Journal*, Vol. 22, April 1984, pp. 478–485.

[4]Fung, K.-Y., "A Simple, Accurate and Efficient Algorithm for Unsteady Transonic Flow," *Recent Advances in Numerical Methods in Fluid Dynamics*, edited by W.G. Habashi, Pineridge Press, Swansea, U.K., 1985.

[5]Fung, K.-Y., Tripp, J., and Goble, B., "Adaptive Refinement with Truncation Error Injection," EES Rept. CFML 84-01, University of Arizona, Tucson, 1984; also *Computer Methods in Applied Mechanics and Engineering*, to be published.

[6]Davis, S. and Malcolm, G., "Unsteady Aerodynamics of Conventional and Supercritical Airfoils," AIAA Paper 80-734, May 1980.

New Eddy Viscosity Model for Computation of Swirling Turbulent Flows

Kwang Yong Kim*
Inha University, Incheon, Korea
and
Myung Kyoon Chung†
Korea Advanced Institute of Science and Technology Seoul, Korea

Introduction

THE conventional k-ϵ model has been widely used to predict relatively simple turbulent flows on the grounds of its simplicity and reasonable accuracy. However, it is well known that the model in its standard form is not adequate for taking into account the secondary straining effect of swirl or buoyancy.

According to Bradshaw,[1] the secondary straining increases or decreases the turbulent length scale in the flowfield depending on the stability of the straining field. In order to make the k-ϵ model adaptable to such flow situations, Launder et al.[2] and Rodi[3] have made one of the model constants in their dissipation equations a function of a Richardson number, which will ultimately change the resulting length scale since $\ell \sim k^{3/2}/\epsilon$. However, both of these forms are only ad hoc models and are not well supported by theory. Obviously, the Reynolds stress model does not require additional modification of the model for these flows.[4] But it requires the solution of a number of differential equations for Reynolds stresses, and the computational cost is prohibitively expensive.

This Note is aimed at proposing a simple theoretical modification of the standard k-ϵ model to solve swirling turbulent flows. The coaxial swirling jet of Ribeiro and Whitelaw[5] and the single swirling round jet of Pratte and Keffer[6] are used to test the performance of the proposed method.

Modification of Eddy Viscosity for Swirling Flow

In the standard k-ϵ model, the eddy viscosity ν_t is given by a function of turbulent kinetic energy k and its dissipation rate ϵ,

$$\nu_t = C_\mu (k^2/\epsilon) \tag{1}$$

where the model constant C_μ is taken as a constant value, $C_\mu = 0.09$. The standard transport equations for k and ϵ in cylindrical coordinates are as follows:

$$U\frac{\partial k}{\partial x} + V\frac{\partial k}{\partial r} = \frac{1}{r}\frac{\partial}{\partial r}\left(r\frac{\nu_t}{\sigma_k}\frac{\partial k}{\partial r}\right) + P - \epsilon \tag{2}$$

$$U\frac{\partial \epsilon}{\partial x} + V\frac{\partial \epsilon}{\partial r} = \frac{1}{r}\frac{\partial}{\partial r}\left(r\frac{\nu_t}{\sigma_\epsilon}\frac{\partial \epsilon}{\partial r}\right) + C_{\epsilon_1}\frac{\epsilon}{k}P - C_{\epsilon_2}\frac{\epsilon^2}{k} \tag{3}$$

where P is the production rate of k,

$$P = \nu_t\left\{2\left[\left(\frac{\partial U}{\partial x}\right)^2 + \left(\frac{\partial V}{\partial r}\right)^2 + \left(\frac{V}{r}\right)^2\right] + \left(\frac{\partial U}{\partial r} + \frac{\partial V}{\partial x}\right)^2 + \left(\frac{\partial W}{\partial x}\right)^2 + \left[r\frac{\partial}{\partial r}\left(\frac{W}{r}\right)\right]^2\right\}$$

and the model constants are $\sigma_k = 1$, $\sigma_\epsilon = 1.22$, $C_{\epsilon_1} = 1.44$, and $C_{\epsilon_2} = 1.92$. The velocity components U, V, and W are in the axial (x), radial (r), and tangential (θ) directions, respectively.

The derivation of our modified eddy viscosity model begins with the following algebraic stress equations[7]:

$$\frac{\overline{u_i u_j}}{k} = \phi_1\frac{P_{ij}}{\epsilon} + \phi_2\delta_{ij} \tag{4}$$

where

$$\phi_1 = \frac{1 - c_2}{(P/\epsilon) + c_1 - 1} \quad \text{and} \quad \phi_2 = \frac{2}{3}\frac{c_2(P/\epsilon) + c_1 - 1}{(P/\epsilon) + c_1 - 1}$$

The constants c_1 and c_2 are inertial and forced return-to-isotropy constants respectively.[8] δ_{ij} is a Kronecker delta, and P_{ij} is the production tensor of the Reynolds stresses $\overline{u_i u_j}$

$$P_{ij} = -\overline{u_i u_k}\frac{\partial U_j}{\partial x_k} - \overline{u_j u_k}\frac{\partial U_i}{\partial x_k}$$

Received Sept. 3, 1986; revision received Dec. 1, 1986.

*Assistant Professor, Mechanical Engineering.
†Associate Professor, Mechanical Engineering.